Structural and Binding Characteristics of the Carboxyl Terminal Fragment of Apolipophorin III from *Manduca sexta*†

Vasanthy Narayanaswami,‡ Cyril M. Kay,§ Kim Oikawa,§ and Robert O. Ryan*,‡

Lipid & Lipoprotein Research Group and Medical Research Council Group in Protein Structure and Function, Department of Biochemistry, University of Alberta, Edmonton, Alberta, Canada T6G 2S2

Received April 29, 1994; Revised Manuscript Received August 31, 1994⊗

ABSTRACT: The molecular basis of the interaction of apolipophorin III (apoLp-III), an exchangeable apolipoprotein from hemolymph of the sphinx moth, *Manduca sexta,* with lipoprotein surfaces and phospholipids was studied by investigating the structural and binding properties of the C-terminal fragment of the native protein. A 4K peptide, corresponding to the terminal helical segment of the native protein, was generated by cyanogen bromide treatment, purified by gel filtration and reverse-phase HPLC, and characterized by N-terminal sequencing and amino acid and mass spectrometric analysis. Circular dichroism (CD) spectroscopy of the peptide in buffer indicated a predominantly unstructured state while addition of trifluoroethanol (TFE), a helix-inducing agent, resulted in an α-helical structure. Sedimentation equilibrium studies revealed that the 4K peptide was monomeric in buffer. The 4K peptide assumed an α-helical conformation in the presence of sodium dodecyl sulfate (SDS) and lysolecithin, but was unstructured in the presence of dimyristoylphosphatidylcholine, either when added to preformed vesicles or upon cosonication, indicating an ability to bind to detergent micelles but not to phospholipid bilayers. Unlike native apoLp-III, the 4K peptide did not confer protection against turbidity development to human low density lipoprotein upon incubation with phospholipase C, indicating an inability to interact with the surface of lipoproteins. Upon interaction with SDS micelles, both the 4K peptide and apoLp-III were resistant to urea-induced denaturation when compared to free apoLp-III, as evaluated by CD spectroscopy. The structural stability conferred upon interaction with detergents was similar for both the peptide and the native protein. Intrinsic fluorescence of the single tyrosine (Tyr) residue (Tyr 145 in the native protein), which is quenched in the free peptide, increased concurrently with the formation of α-helix in the presence of TFE or detergents. Tyr fluorescence emission was followed in both native apoLp-III and the 4K peptide as a probe to monitor conformational changes in different environments such as in H_2O, ^2H_2O, TFE, and detergent micelles. Our studies suggest that other domains in the protein play a role in the amphipathic helix forming capacity of the terminal helical region of apoLp-III. Further, the fluorescence status of Tyr can be used as a reliable probe to monitor the conformational changes that take place upon binding to apolar surfaces.

Apolipophorin III (apoLp-III)[1] from the sphinx moth, *Manduca sexta*, plays a critical role in transport of lipoprotein-associated diacylglycerol in hemolymph during sustained flight (Ryan, 1990; Van der Horst, 1990). ApoLp-III is a water soluble protein present in abundance in the hemolymph. A structural scaffolding role has been assigned to apoLp-III as it associates with the expanding hydrophobic surface of low density lipophorin during lipid loading (Wells et al., 1987), thereby stabilizing the lipoprotein particle.

The primary sequence of apoLp-III, which lacks tryptophan and cysteine, consists of 166 amino acid residues and is nonglycosylated (Cole et al., 1987; Kawooya et al., 1984). While the tertiary structure of *M. sexta* apoLp-III is not known, secondary structure predictions suggest that the protein contains sequentially-located amphipathic α-helical segments of variable length. An analogous apoLp-III from *Locusta migratoria*, which bears considerable sequence and functional homology (Van der Horst et al., 1988), has been crystallized (Holden et al., 1988), and X-ray crystallographic studies at 2.5 Å reveal a bundle of five amphipathic helices connected by loops (Breiter et al., 1991).

The amphipathic helix has been identified as the putative lipid-associating motif in exchangeable apolipoproteins and has long been proposed to be the determining factor of lipid binding ability (Segrest et al., 1974), though there is considerable debate as to the structural motifs involved in the binding of apolipoproteins to lipids. In general, the apolar face of the helix was suggested to be buried in the lipid milieu, with the polar face exposed to the solvent and available for interaction with the charged phospholipid headgroups. X-ray crystallographic studies of lipid-free *L. migratoria* apoLp-III (Breiter et al., 1991) indicated that the

† This work was supported by grants from the Medical Research Council and the Alberta Heart and Stroke Foundation.

* To whom correspondence should be addressed, at the Lipid & Lipoprotein Research Group, 328 Heritage Medical Research Building, University of Alberta, Edmonton, Alberta, Canada T6G 2S2. FAX: 403-492-3383.

‡ Lipid & Lipoprotein Research Group.

§ Medical Research Council Group in Protein Structure and Function.

⊗ Abstract published in *Advance ACS Abstracts,* October 15, 1994.

[1] Abbreviations: apo, apolipoprotein; apoLp-III, apolipophorin III; CD, circular dichroism; DLPC, dilauroylphosphatidylcholine; DMPC, dimyristoylphosphatidylcholine; LDLp, low density lipophorin; LDL, low density lipoprotein; PL-C, phospholipase C; TFE, trifluoroethanol; HPLC, high-pressure liquid chromatography; Trp, tryptophan; Tyr, tyrosine.

0006-2960/94/0433-13312$04.50/0

five amphipathic helices orient in such a way that their hydrophobic faces are juxtaposed, facing away from the solvent while their hydrophilic sides are exposed to the solvent. It was proposed that a large conformational change occurs in the presence of lipids with an opening of the helix bundle at loop regions between helices 2 and 3, and 4 and 5, so that their hydrophobic sides now face the lipid, facilitating binding. Further, it has been postulated that ionic interactions may play a critical role in initiating and stabilizing the binding of apoLp-III with phospholipid surfaces (Zhang et al., 1993). Such a conformational flexibility could possibly explain the dichotomous existence of apoLp-III in free and lipid-bound states.

A number of studies have been undertaken with mammalian apolipoprotein fragments and synthetic peptide analogs, and there is a general lack of consensus with regard to the structural basis of lipid binding. In human apoC-II and apoE, amphipathic segments toward the carboxyl terminus appear to be involved in phospholipid binding (Sparrow & Gotto, 1980; Sparrow et al., 1985). In human apoA-II and in apoC-I, the phospholipid-associating domains were found to reside at opposite ends of the proteins, with contributions from helical segments in both the carboxyl and amino terminal ends [see Segrest et al. (1992) and references cited therein]. In human apoA-I, despite the presence of amphipathic segments throughout the length of the protein, the phospholipid-binding domain appears to be on multiple sites toward the carboxyl terminus (Sparrow & Gotto, 1980).

In *M. sexta* or *L. migratoria* apoLp-III little is known of the mechanism of protein−lipid interactions, though there is evidence that large conformational changes take place when the protein binds to phospholipid particles (Wientzek et al., 1994; Weers et al., 1994). As the carboxyl terminus appears to be involved in lipid association in many apolipoproteins [see Segrest et al. (1992)], we studied, for the first time, the properties of a 36-residue carboxy terminal peptide (4K peptide) that corresponds to the fifth helical segment of native *M. sexta* apoLp-III. The presence of a single Tyr residue in this segment and in the native protein (Tyr 145) was useful as a fluorescent probe to monitor conformational changes and lipid interaction. We report here the studies on the structural characteristics of the 4K peptide in aqueous, detergent, and phospholipid environments using CD and fluorescence spectroscopy and functional aspects using lipoprotein and diacylphospholipid binding assays.

MATERIALS AND METHODS

Materials. Cyanogen bromide, dimyristoylphosphatidylcholine, egg yolk L-α-lysolecithin, sodium dodecyl sulfate, trifluoroethanol, ^2H_2O, and phospholipase C from *Bacillus cereus* were obtained from Sigma Chemical Co.

Apolipophorin III Purification and LDL Isolation. ApoLp-III was purified from the hemolymph of adult *M. sexta* as described previously (Wells et al., 1985) with some modifications as outlined by Wientzek et al. (1994). LDL (density 1.006−1.063 g/mL) was isolated from fasting human plasma by sequential density ultracentrifugation (Schumaker & Puppione, 1986) and stored under argon at 4 °C.

Cyanogen Bromide Digestion and Purification of 4K Peptide. Purified apoLp-III was dissolved in 70% formic acid at a concentration of 25 mg/mL and treated with a 100-fold molar excess of cyanogen bromide per methionine residue. The mixture was incubated for 18 h at room temperature followed by addition of excess water and lyophilization. The digestion was followed by Tricine−SDS−polyacrylamide gel electrophoresis used for separation of low molecular weight peptides (Schägger & von Jagow, 1987). The dried residue was dissolved in a minimal volume of 20 mM sodium phosphate buffer, pH 7.0, containing 150 mM sodium chloride and 1 mM EDTA (FPLC buffer) and centrifuged. The supernatant was loaded on a Superose 12 FPLC gel filtration column which was previously equilibrated with FPLC buffer and eluted at a flow rate of 0.5 mL/min. The fractions were analyzed by an analytical reverse-phase C-8 column (Zorbax 300SB-C8, 2.1 mm × 15 cm) using a Hewlett-Packard HP 1090 liquid chromatograph, with a linear AB gradient of 2% B/min, where solvent A was 0.05% trifluoroacetic acid in water and solvent B was 0.05% trifluoroacetic acid in acetonitrile. Fractions were monitored at 220 nm, and those containing the 4K peptide (retention time: 19.5 min; verified by N-terminal sequencing) were pooled, desalted on a preparative HPLC column, and eluted with a linear gradient of acetonitrile at 2%/min. The fractions were further analyzed by analytical HPLC, and those containing the pure 4K peptide (>99% pure) were pooled and lyophilized.

Characterization of the 4K Peptide. The criteria of purity of the 4K peptide was established by HPLC and amino acid analysis. N-Terminal sequencing of the peptide revealed the sequence Glu-Glu-Thr-Asn-Lys, as established earlier (Cole et al., 1987). Mass spectrometric analysis was performed on a VG Biotech (Fisons Instruments) mass spectrometer by platform electrospray ionization.

Sedimentation Equilibrium. Hydrodynamic studies on the 4K peptide were carried out on a Beckman Model E analytical ultracentrifuge equipped with electronic speed control, RTIC temperature control, and titanium rotor. Molecular weight determinations were performed at 20 °C using the sedimentation equilibrium techniques described by Chervenka (1969). The 4K peptide was run at a concentration of 1 mg/ml in 10 mM Tris/100 mM KCl, pH 8.0, at a speed of 44 000 rpm using the Rayleigh interference optical system and at 1.8 mg/mL in 50% TFE in the same buffer at 52 000 rpm using the photoelectric scanner optical system for 48 h. The partial specific volume of the peptide was assumed to be 0.73 and the ln y versus r^2 data were fitted to a second-order polynomial equation, and apparent weight average molecular weights were calculated from the slopes of the plots.

Peptide−Diacylphospholipid Interaction Studies. The ability of the 4K peptide to disrupt and transform preformed multilamellar bilayer vesicles into disc-like peptide−lipid complexes was determined by electron microscopy and circular dichroism spectroscopy (CD) in a manner analogous to that described for the native protein (Wientzek et al., 1994). Dimyristoylphosphatidylcholine (DMPC) vesicles were mixed with the 4K peptide or control apoLp-III (2 mg/mL) solution in 0.2 M Tris-HCl, pH 7.2, containing 8.5% potassium bromide and 0.01% EDTA (buffer A), to give final lipid:peptide molar ratios varying from 70:1 to 1:1, and incubated at 24 °C for 18 h. The mixture was subjected to density gradient ultracentrifugation to determine association of peptide with diacylphospholipids. The density of the incubation mixture was adjusted to 1.21 g/mL with KBr to a final volume of 2.5 mL, overlaid with 0.9% saline in a 5

mL Quick-Seal tube, and centrifuged at 65 000 rpm for 3 h at 4 °C. Following centrifugation, the tube was fractionated from the top in 0.5 mL aliquots and phospholipid assay was carried out using an enzymatic kit (Wako Pure Chemical Industries, Ltd., Japan). Fractions containing DMPC/4K peptide or DMPC/apoLp-III complexes were examined under an electron microscope. Native PAGE was carried out as described by Ryan et al. (1985) for DMPC/apoLp-III complexes. Alternatively, the 4K peptide was subjected to cosonication with DMPC according to the protocol of Lund-Katz et al. (1990). DMPC was dried under nitrogen as a thin film from $CHCl_3/CH_3OH$ solutions (3:1 v/v) and further dried under vacuum for about 2 h. The 4K peptide in 150 mM NaCl/1 mM EDTA, pH 8.0, was added to the film to give a final lipid:peptide weight ratio of 2.5:1 and bath sonicated at 24 °C for about 10 min until clear. A parallel control experiment was performed with native apoLp-III.

CD Spectroscopy. CD studies were carried out at a peptide concentration of 1 mg/mL in 0.1 M sodium phosphate buffer, pH 7.0, on a Jasco J-720 spectropolarimeter (Jasco Inc., Easton, MD) interfaced to an Epson Equity 386/25. The instrument was calibrated using ammonium *d*-(+)-10-camphorsulfonate at 290.5 and 192 nm and with *d*-(−)-pantoyllactone at 219 nm. CD spectra were collected under different conditions such as in 0.1 M phosphate buffer, pH 7.0, in the presence of 50% trifluoroethanol (TFE) (v/v), 0.4% egg lysolecithin (lysoPC), and 1% SDS and in different lipid:peptide ratios.

Fluorescence Measurements. Fluorescence emission of Tyr in both the 4K peptide and native apoLp-III was monitored at an excitation wavelength of 277 nm, and the emission was scanned from 270 to 350 nm using a Perkin-Elmer MPF-44B spectrofluorometer with the temperature maintained at 20 °C in a thermostated cell holder. The excitation and emission bandwidths were 8 and 10 nm, respectively. The quantum yield of Tyr in native apoLp-III and the 4K peptide was calculated and compared with that of free Tyr. Quantum yield is defined as the the ratio of photons emitted to the photons absorbed and was calculated according to Eisinger (1969) as:

$$Q_u = (Q_s A_u)(OD_s)/(A_s)(OD_u)$$

where Q_u is the quantum yield of the unknown, Q_s is the quantum yield of standard (Tyr in phosphate buffer, pH 7.0, calculated as 0.07), A_u is the area under the emission spectrum of the unknown, A_s is the area under emission spectrum of Tyr, OD_u is the optical density of the unknown at 277 nm (excitation wavelength of Tyr), and OD_s is the optical density of Tyr at 277 nm.

Peptide−Lipoprotein Interactions. Phospholipase C (PL-C) has been shown to induce aggregation of human LDL (Suits et al., 1989) through loss of surface phospholipid. The aggregation process is prevented, however, when incubations of LDL and PL-C include exchangeable apolipoproteins (including apoLp-III and human apoA-I), which apparently serve as substitute surface components on the phospholipid-depleted lipoprotein (Liu et al., 1993). The ability of the 4K peptide to prevent PL-C-induced LDL aggregation and turbidity development has been used as an assay system to monitor association with lipoprotein surfaces. The assay mixture contained 20 μg protein of human LDL in 50 mM Tris-HCl, pH 7.5, containing 150 mM NaCl and 2 mM $CaCl_2$ at 37 °C in a final volume of 250 μL in a microtiter plate. ApoLp-III (20 μg) or the 4K peptide (20 μg) in the same buffer was added, and the reaction was started by the addition of 400 milliunits of PL-C. The absorbance was monitored at 340 nm in a microtiter plate reader (SLT Labinstruments) to measure the onset of sample turbidity as a function of time.

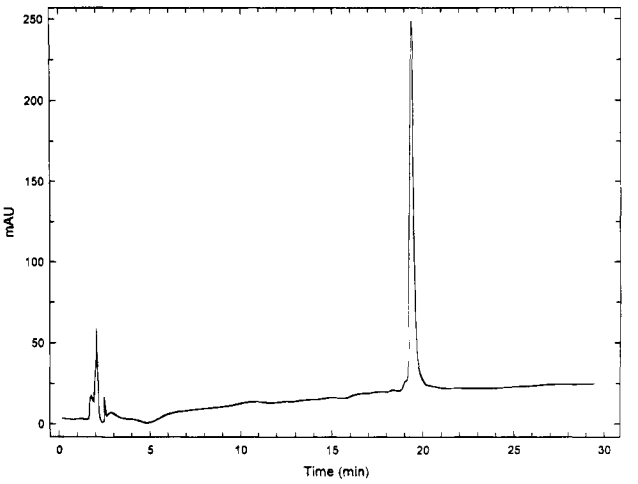

FIGURE 1: The purified 4K peptide after the preparative HPLC step elutes with a retention time of 19.5 min on a C-8 Zorbax analytical reverse-phase HPLC column (Zorbax 300SB, 2.1 mm × 15 cm) with a linear AB gradient of 2% B/min, where solvent A was 0.05% trifluoroacetic acid in water and solvent B was 0.05% trifluoroacetic acid in acetonitrile. The eluent was monitored at 220 nm.

Electron Microscopy. Electron microscopy was performed in a Philips EM420 operated at 100 kV as described earlier (Weintzek et al., 1994). The samples were adsorbed on a carbon-coated grid, washed three times with 10 mM Tris, 10 mM NaCl, and 1.5 mM $MgCl_2$, and negatively stained with 2% sodium phosphotungstate, pH 7.0.

Effect of Urea on SDS/Peptide and SDS/ApoLp-III Mixed Micelles Using CD Spectroscopy. Lipid-free apoLp-III or apoLp-III and 4K peptide in 1% SDS micelles were treated with urea up to a final concentration of 6.5 M (25 °C for apoLp-III and 35 °C for the peptide), and the relative ellipticities (θ) at 220 nm were determined by CD spectroscopy at various urea concentrations.

Secondary Structure Predictions and Sequence Alignment. The C-terminal sequences of apoLp-III from *L. migratoria* (Gln 125 to Asn 161) and *M. sexta* (Glu 131 to Gln 166) were analyzed by the SEQSEE program (Wishart et al., 1994), a multipurpose suite of programs, for secondary structure identification and sequence alignment. The crystal structure of *L. migratoria* apoLp-III (Breiter et al., 1991) was used as a guideline for evaluating strategies for cleavage of the terminal helix of *M. sexta* apoLp-III.

RESULTS

Purification and Characterization of the 4K CNBr Fragment. CNBr-generated fragments of apoLp-III were separated by FPLC, and fractions containing the 36-residue carboxyl terminal fragment were purified by HPLC (Figure 1). The cleavage was only partial as evidenced by polyacrylamide gel electrophoresis (not shown) of the total digest, possibly due to the presence of a glutamate residue following both Met 12 and Met 130. The product was >99% pure, and its identity was confirmed by N-terminal sequencing and

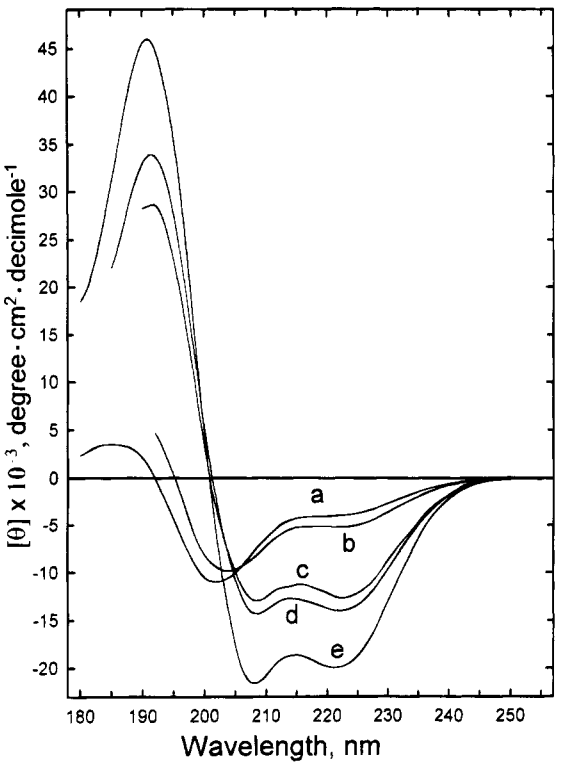

FIGURE 2: CD spectra of the 4K peptide at a concentration of 1 mg/mL were recorded in 100 mM sodium phosphate buffer, pH 7.0, curve a; in the presence of DMPC at a lipid:peptide mole ratio of 15:1, curve b; in 0.4% lysoPC, curve c; in 1% SDS, curve d; and in 50% TFE in phosphate buffer, curve e.

amino acid analysis. Mass spectrometric analysis showed the mass to be 4197 ± 2 daltons (calculated mass was 4196 daltons).

Analytical Ultracentrifugation. Sedimentation equilibrium studies of the 4K peptide were carried out to assess its physical state in aqueous buffer and in 50% TFE (not shown). The plot of ln y versus r^2 was linear in both environments, and the apparent molecular mass of the peptide was calculated to be 4110 and 4990 daltons in buffer and 50% TFE respectively, clearly suggesting the presence of a single species corresponding to a monomer.

CD Studies. The CD spectra of the 4K peptide in buffer (curve a) revealed that the fragment exists in a predominantly random coil, unstructured state (Figure 2). Upon progressive addition of TFE up to 50% (v/v), there was a corresponding increase in negative ellipticity at 222 nm, reflecting an increase in α-helical conformation in the peptide (data shown only for 50% TFE, curve e). Previous studies have shown that the lipid-free form of native apoLp-III has an α-helical content of ~60% (Kawooya et al., 1986; Ryan et al., 1993) which increases essentially to 100% upon association with DMPC (Wientzek et al., 1994). When a similar study was undertaken with the 4K peptide using DMPC or dilauroylphosphatidylcholine (data not shown), there was minimal induction of secondary structure (curve b). Upon cosonication with DMPC, the peptide failed to adopt an α-helical structure even though the solution was clear after sonication. However, when detergent micelles of lysoPC and SDS were used (curves c and d, respectively) to simulate the apolar environment of lipid bilayers of membranes (Snel et al., 1991; Macquaire et al., 1993; Roth et al., 1989), the 4K peptide did adopt an α-helical conformation, indicating an interaction with micelles.

Fluorescence Measurements. Quantum yield of Tyr fluorescence in native apoLp-III and 4K peptide was evaluated under varying conditions to investigate the conformational changes taking place and to assess the overall microenvironment of the single Tyr residue (Figure 3 and Table 1). Free Tyr was used as a control. The quantum yields of Tyr in native apoLp-III and in the 4K peptide are 0.012 and 0.037, respectively, in buffer (panel A), which is significantly less than the value observed for free Tyr in buffer (0.07; Table 1). This indicates quenching of the intrinsic fluorescence and, in general, can be attributed to hydrogen bonding of the phenolic hydroxyl proton (Lakowicz, 1983). In order to determine if proton transfer to solvent was taking place (Stryer, 1966), quantum yields of Tyr in both the native protein and the peptide were assessed after extensive exchange of the samples with ^2H_2O (panel B). The quantum yields increased by about 42% and 35% for the native protein and peptide, respectively (Table 1). In 50% TFE (Figure 3, panel C; Table 1), the quantum yield of Tyr in 4K peptide increased 3-fold (data not shown for 5%, 10%, 20%, and 30% TFE, which showed a progressive increase in fluorescence) with a concurrent induction of α-helix (Figure 2). However, for apoLp-III, a 10-fold increase in quantum yield was observed in 50% TFE. In control experiments, a modest increase in quantum yield of free Tyr in 50% TFE to 0.089 (~25%) was observed. Upon interaction of the 4K peptide with lysoPC, yielding mixed micelles (Figure 3, panel D; Table 1), the quantum yield of Tyr increased 3.6-fold, while an even larger increase was registered with apoLp-III (~13-fold). Unlike native apoLp-III (Wientzek et al., 1994), no change was observed in the quantum yield of Tyr in the 4K peptide in the presence of DMPC (data not shown), complementing the CD studies which indicate a lack of binding.

Interaction of 4K Peptide with Lipoproteins and Phospholipid Bilayers. CD and fluorescence studies showed that the 4K peptide possesses the ability to form α-helix in TFE and when bound to detergent micelles. Thus, *a priori*, it may appear that the peptide may exhibit an affinity toward lipoprotein surfaces. The 4K peptide and native apoLp-III were compared for their ability to protect human LDL from turbidity development upon incubation with PL-C. Figure 4 is a plot of sample absorbance as a function of time following the addition of PL-C. In the absence of PL-C, LDL is stable, as seen by the lack of turbidity development, while in the presence of PL-C turbidity develops following an initial lag phase. Exogenous native apoLp-III (20 μg) provided excellent protection against PL-C-induced turbidity development and was practically indistinguishable from the negative control without PL-C. The 4K peptide, on the other hand, was not effective in preventing aggregation, suggesting an inability to interact with the lipoprotein surface. Increasing the concentration of the peptide up to 150 μg also failed to provide protection (data not shown) and, in fact, was slightly detrimental at these levels, causing more turbidity than the positive control.

Similarly, the ability of the 4K peptide to disrupt vesicular structures and form disc-like complexes was studied. Multilamellar vesicles were prepared by sonication of a suspension of DMPC in buffer, which upon addition of native apoLp-III at a lipid:protein molar ratio of 67:1 formed disc-like structures (Wientzek et al., 1994). However, addition of the 4K peptide under similar conditions at lipid:peptide

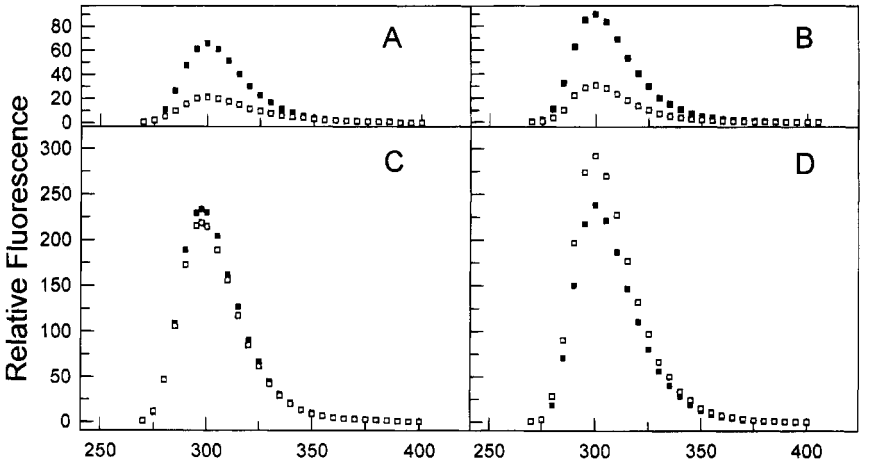

FIGURE 3: Tyr fluorescence emission of native apoLp-III (open squares) and the 4K peptide (closed squares) was monitored at an excitation wavelength was 277 nm, and the emission was scanned from 270 to 350 nm; the excitation and emission slit widths were 8 and 10 nm, respectively. Fluorescence emission was monitored in different environments as follows: (panel A) 100 mM sodium phosphate buffer, pH 7.0; (panel B) ^2H_2O; (panel C) 50% TFE; and (panel D) 0.4% lysoPC.

Table 1: Quantum Yield of Tyr in the Free State, in ApoLp-III, and in the 4K Peptide[a,b]

	H_2O	^2H_2O	50% TFE	1% SDS
free Tyr	0.070	—[c]	0.089	0.070
native apoLp-III	0.012	0.017	0.120	0.171
4K peptide	0.037	0.050	0.128	0.180

[a] Quantum yield was determined as described under Materials and Methods, according to Eisinger (1969). [b] Quantum yield was determined in 50 mM sodium phosphate, pH 7.0, containing 100 mM NaCl for all except ^2H_2O data. [c] Stryer (1966) reported a 25% increase in quantum yield of free Tyr in ^2H_2O.

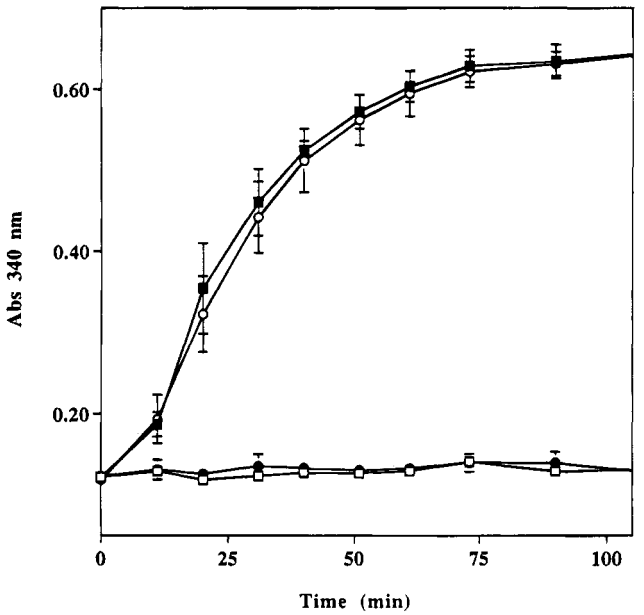

FIGURE 4: Effect of apoLp-III and 4K peptide on PL-C-induced aggregation of human low density lipoprotein. The assay mixture consisted of 20 μg of LDL protein in 50 mM Tris-HCl buffer, pH 7.5, containing 150 mM NaCl and 2 mM $CaCl_2$ at 37 °C; the reaction was started by the addition of 400 milliunits of PL-C. Controls, without PL-C (open squares) and with PL-C (closed squares), were carried out. ApoLp-III (20 μg) (closed circles) and the 4K peptide (20 μg) (open circles) were included before addition of PL-C. Turbidity was monitored at 340 nm in a microtiter reader.

molar ratios ranging from 70:1 to 1:1 did not result in disc formation as judged by electron microscopy of both the incubation mixture and following density gradient ultracentrifugation (not shown). Also, when the peptide was cosonicated with DMPC, it did not form discs. Native PAGE of the mixture (not shown) also failed to show bands corresponding to DMPC/peptide complexes.

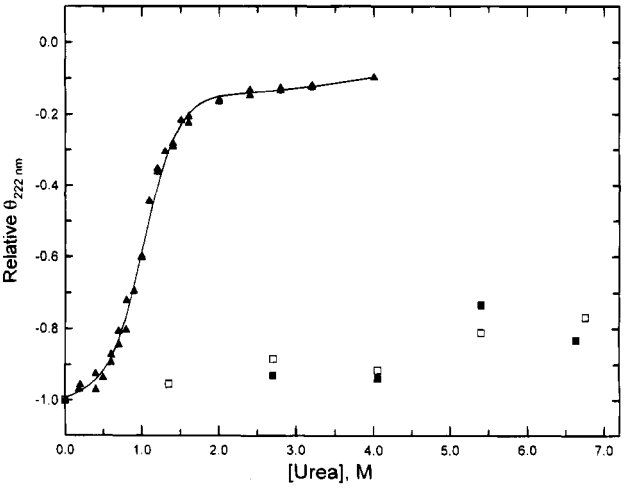

FIGURE 5: Effect of urea on the secondary structural stability of lipid-free apoLp-III, SDS micelle-bound apoLp-III, and 4K peptide. The SDS micelle-bound peptide (closed squares) and SDS micelle-bound apoLp-III (open squares) were incubated with increasing concentrations of urea, and the relative ellipticity at 222 nm was monitored. The final concentration of SDS was 1%, while that of the peptide and apoLp-III was about 0.5 mg/mL in 100 mM phosphate buffer, pH 7.0. Also shown is the denaturation profile of lipid-free, native apoLp-III (closed triangles), with a midpoint of denaturation around 1 M urea.

Effect of Urea on SDS/Peptide and SDS/ApoLp-III Mixed Micelles. In an effort to determine if the inability of the peptide to bind to diacylphospholipid bilayers and lipoprotein surfaces may be explained on the basis of the strength of the binding interaction, mixed-micelle complexes of SDS and peptide or apoLp-III were exposed to increasing concentrations of urea (Figure 5). Changes in secondary structure were followed by CD spectroscopy, and the relative ellipticity at 222 nm is plotted as a function of urea concentration. As a control, the denaturation profile of the lipid-free, native apoLp-III was performed and the half-maximal concentration of urea required for denaturation was found to be 1 M. However, when present as mixed micelles with SDS, both apoLp-III and the 4K peptide possessed about

60% of the native ellipticity at 6.5 M urea. This suggests that association with detergents confers stability to both the protein and the peptide.

DISCUSSION

The molecular basis of interaction of *M. sexta* apoLp-III with lipid particles was assessed by examining the structural and binding properties of its terminal 36-residue fragment (Glu 131 to Gln 166). CNBr cleavage at Met 130 yielded a 4K C-terminal peptide, which enabled us to investigate if this segment can serve as a structural or functional unit of the native protein. When the primary sequences of the corresponding apoLp-IIIs from *L. migratoria* and *M. sexta* were aligned using the SEQSEE program (Wishart et al., 1994), they showed a high degree of sequence similarity, taking into consideration the helical propensities of the residues involved. Further, it was determined that the C-terminal fragment generated in this study encompasses the entire fifth helical segment of apoLp-III from *L. migratoria* (Gln 125 to Asn 161) (Breiter et al., 1991). Consistent with the known helical content of *L. migratoria* apoLp-III, secondary structure predictions suggest that the 4K peptide from *M. sexta* apoLp-III has the propensity to form an amphipathic α-helix.

In contrast to native apoLp-III, which has the ability to bind to lipoprotein surfaces and to transform phospholipid bilayers to discs, the 4K peptide did not possess this function and assumed a random coil structure both in buffer alone or in buffer containing diacylphospholipids. However, the peptide adopted an α-helical conformation in 50% TFE and upon incubation with detergent micelles, including lysophosphatidylcholine and SDS. It has been shown that binding of SDS to polypeptides induces secondary structure formation (Jirgensons, 1976; Su & Jirgensons, 1977) and the micellar environment resembles the apolar lipid assembly of membranes (Roth et al., 1989), thereby making detergent micelles a reasonably good mimic for these studies.

In lipoprotein binding assays designed in our laboratory using PL-C, it was shown that apoLp-III prevents onset of aggregation of human LDL (Liu et al., 1993) or insect lipoproteins (Singh et al., 1994) by binding to the exposed hydrophobic surfaces created by hydrolysis of phospholipid headgroups. In LDLp it was rationalized (Wang et al., 1992) that apoLp-III intercalates between phospholipid molecules and interacts with diacylglycerol at the particle surface, following opening of the helix bundle and exposure of its hydrophobic core. The 4K peptide, on the other hand, was found to be nonfunctional in terms of binding to LDL, even when present in excess. This is consistent with the lack of binding of the peptide to model phospholipid bilayers. Taken together, the data suggest that other segments of the apoLp-III molecule participate in these lipid binding interactions or that more structural elements from the rest of the molecule are required to impart binding capability to this segment.

Fluorescence Studies. Measurement of intrinsic Tyr fluorescence can be used to obtain potentially useful structural information, though unlike tryptophan, the λ_{max} of Tyr emission is relatively insensitive to the polarity of the solvent (Lakowicz, 1983). We have taken advantage of the sensitivity of the quantum yield of intrinsic fluorescence of the single Tyr residue (Tyr 145 of native apoLp-III; the protein lacks Trp) to the surrounding environment and have used it as a probe to monitor conformational changes involved in protein/peptide binding to apolar surfaces. It was shown earlier that interaction with DMPC results in a 10-fold enhancement of apoLp-III Tyr fluorescence (Wientzek et al., 1994). In the homologous *L. migratoria* apoLp-III, it has been proposed that the five-helix bundle can open at hinge regions, enabling interaction of the exposed hydrophobic surface with lipid particles (Breiter et al., 1991). Based on this model it was suggested by Weintzek et al. (1994) that, for *M. sexta* apoLp-III, enhancement of Tyr fluorescence in the lipid-bound state was due to a similar opening. By isolating the fifth helical segment containing Tyr 145, this phenomenon was studied in more detail.

The remarkable perturbations in Tyr fluorescence profile and quantum yields in aqueous buffer, TFE, and detergent micelles are indicative of the differences in secondary structure and in the Tyr microenvironment in both the peptide and the native protein [see Lakowicz (1983)]. In native apoLp-III, the quantum yield of Tyr is low (a common phenomenon in many proteins; Teale, 1960), which suggests quenching of fluorescence due to hydrogen bonding of the phenolic hydrogen (Lakowicz, 1983). Quenching may be due to proton transfer to the solvent (Stryer, 1966), or H-bonding to the side chain functional groups of proximal residues or to the peptide backbone (Edelhoch et al., 1968; Cowgill, 1963). H-bonding of the phenolic hydrogen renders it nonfluorescent and may occur due to proton transfer during the ground or excited state lifetime to a proximal carboxyl or amino group (Edelhoch et al., 1968).

The relatively low quantum yield observed for the 4K peptide in aqueous buffer is possibly due to intrinsic quenching from proximal residues in the various conformers of the random coil state. However, since the quantum yield is higher than that observed for the native protein, the data suggest a less restricted environment for the fluorophore in the former. The small increase in quantum yield (~40%) for both the peptide and native protein when present in ^2H_2O indicates only a minor contribution to quenching due to proton transfer reactions with the solvent (Stryer, 1966). The single Tyr residue of apoLp-III is present on the nonpolar face of the fifth amphipathic helix (see Figure 6) and is therefore probably located in the interior of the molecule in the native lipid-free protein, facing away from the solvent. Such a position would enable H-bonding of the phenolic hydrogen to a residue located in one of the other four helices. Titration of 4K peptide with TFE resulted in a progressive enhancement of tyrosine fluorescence corresponding to the increase seen in α-helicity, thereby further diminishing the possibility that the quenching moiety resides on the same helix as proposed earlier (Ryan et al., 1993). Sedimentation equilibrium studies clearly indicate a lack of oligomerization of the peptide both in the native state and when present as a helix, thereby eliminating the possibility that quenching occurs via interaction with neighboring peptide molecules.

When full-length apoLp-III is present in 50% TFE, the increase in α-helicity (Ryan et al., 1993) is accompanied by a 10-fold increase in Tyr quantum yield (Table 1). This may be rationalized by the nature of interaction of TFE with the protein (Sönnichsen et al., 1992); the hydrophobicity of TFE matches that of the interior of the protein and, therefore, alters its tertiary structure by destabilizing the hydrophobic interactions (Lau et al., 1984). Occupation of the accessible sites in the interior of the helix bundle by TFE may cause partial

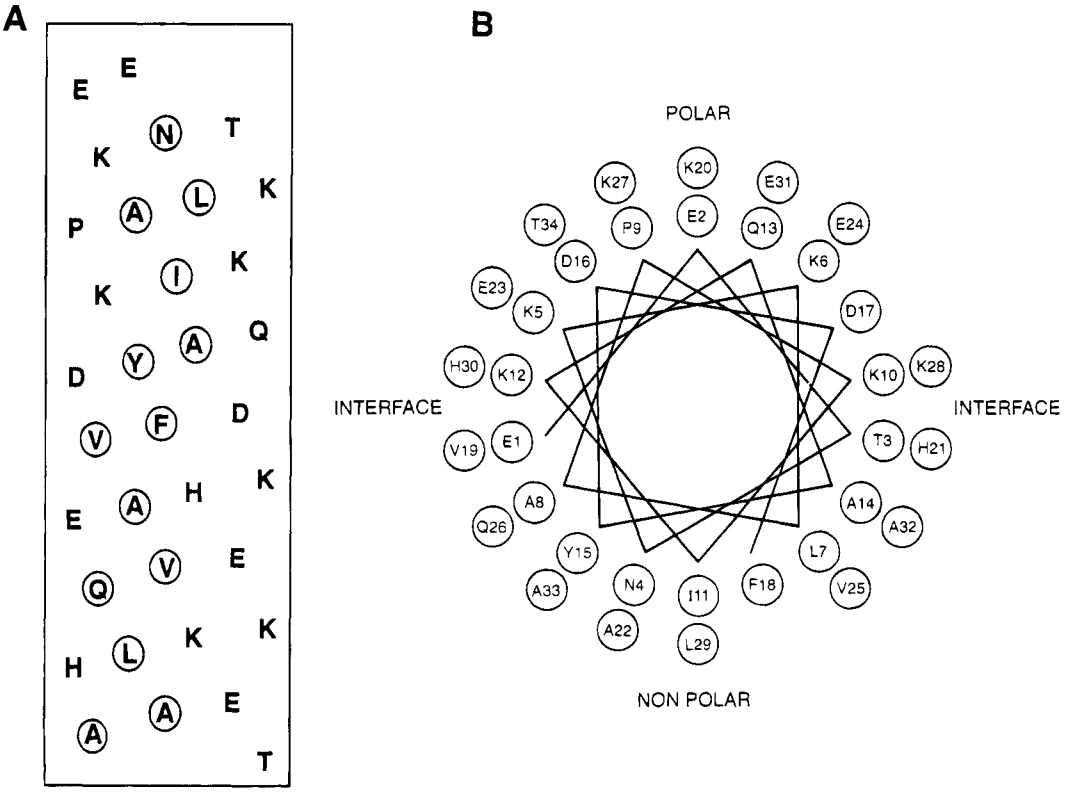

FIGURE 6: Secondary structure predictions of the 4K peptide as determined by the software package SEQSEE (Wishart et al., 1994) revealed an α-helical structure with a high degree of sequence and secondary structural similarity with the corresponding segment from *L. migratoria* (Gln 125 to Asn 161) . The 4K peptide is represented as a helical net (from Glu 131 to Thr 164), where the nonpolar residues are circled, in panel A. Helical wheel representation of the 4K peptide (Glu 131 to Gln 166) is depicted in panel B, showing the polar and nonpolar faces and the interface. Standard amino acid single letter codes were used (A, alanine; D, aspartate; E, glutamate; F, phenylalanine; H, histidine; I, isoleucine; K, lysine; L, leucine; N, asparagine; P, proline; Q, glutamine; S, serine; T, threonine; V, valine; W, tryptophan).

opening at the hinge domains, resulting in disruption of H-bonding interactions of the phenolic moiety, thereby offering an explanation for the decrease in intrinsic quenching. The same quantum yield values obtained for both the protein and peptide in 50% TFE suggest that the structural organization of the peptide resembles that of the C-terminal domain of the protein. These observations indicate that Tyr fluorescence can be used to monitor structural changes involved in the protein and lend credence to the hinged-opening hypothesis (Breiter et al., 1991). It is envisaged that reorientation of a quenching moiety residing in either helix 3 or 4 results in it moving away from the sphere of contact with the fluorophore. The marked increase in fluorescence quantum yield for both the native protein and peptide in the presence of detergent micelles indicates binding to micellar complexes. The absolute value of quantum yield is the same for both the native protein and the peptide (Table 1), suggesting a similar microenvironment for Tyr in the micelle-bound state.

Factors Influencing Lipid Binding Characteristics of Proteins/Peptides. In a minimalist approach, when synthetic model peptides were examined, it was noted that several factors influenced the ability of amphipathic helix-forming peptides to bind to lipids [see Segrest et al. (1992) and references cited therein]. They included the degree of amphipathicity of the peptide (Kanellis et al., 1980), length of the fragment (McLean et al., 1991; Vanloo et al., 1991), the number of helices involved (Jonas et al., 1993), cooperativity between helices (Anantharamaiah et al., 1985), and the hydrophobicities and the topological distribution of charges on the helical surface (Kanellis et al., 1980; Anantharamaiah et al., 1985; Epand et al., 1987). Further, the exchangeable apolipoproteins were found to have amphipathic helical domains that fall into three classes, termed A, G*, and Y (Segrest et al., 1990, 1992). The class A amphipathic helices are characterized by the presence of negatively charged residues in the center of the polar face, and a cluster of positively charged residues at the polar–nonpolar interface, the latter apparently apposed to the negatively charged phosphate groups of the phospholipid, and the former juxtaposed to the positively charged amino groups of choline. The alkyl side chains of the charged residues at the polar–nonpolar interface are thought to enhance the hydrophobicity of the nonpolar face. This forms the basis of the "snorkel hypothesis" proposed earlier (Segrest et al., 1992). A correlation has been made between the lipid affinity and the extent to which an amphipathic helical segment fits into a class A snorkel motif since there is a large degree of variability in the binding affinities of different apolipoproteins and within different segments in an apolipoprotein. The class G* helices (similar to those found in globular proteins) are characterized by a random radial arrangement of positive and negatively charged residues while class Y helices have the charged amino acids arranged in a "Y" motif. In order to probe the significance of the topological distribution of charges in class A peptides, Kanellis et al. (1980) designed peptides with the appropriate distribution of charges which were shown to exhibit lipid-binding abilities. On the other hand, synthetic peptides with a reversed distribution of charges had diminished lipid-binding affinities when compared to the parent peptide (Kanellis et al., 1980). However, the lipid-binding property

Table 2: Comparison of the Hydrophobic Moment and Hydrophobicity Values of the 4K Peptide with Those of Other Amphipathic Helices in Insect ApoLp-III

residues in apolipoprotein	mean hydrophobic moment per residue[a]	mean hydrophobicity per residue of nonpolar face[b]
M. sexta apoLp-III[c]		
residues 9−31	0.515	0.441
residues 72−88	0.485	0.453
residues 131−164	0.475	0.364
L. migratoria apoLp-III[d]		
helix 1 (8−30)	0.487	0.732
helix 5 (131−158)	0.424	0.550

[a] Mean hydrophobic moment per residue was calculated using the normalized consensus hydrophobicity scale of Eisenberg et al. (1984). [b] Mean hydrophobicity of the nonpolar face per residue was calculated based on the helical net diagram using the normalized consensus hydrophobicity scale of Eisenberg et al. (1984). [c] Secondary structure prediction of *M. sexta* apoLp-III was carried out using the software SEQSEE (Wishart et al., 1994) which yields a consensus prediction based on different algorithms; an α-helical structure was predicted from residue 131 to 164 in the 4K peptide. Alignment of the primary sequence of apoLp-III from *M. sexta* and *L. migratoria* was also carried out using the same program. Residues 9−31 and 72−88 of *M. sexta* apoLp-III have been predicted to correspond to helices 1 and 3 of *L. migratoria* apoLp-III, respectively, while residues 131−166 (4K peptide) correspond to part of the loop preceding helix 5 and the entire fifth helix of *L. migratoria* apoLp-III, according to the model structure of *M. sexta* apoLp-III generated by Dr. Wang et al. (University of Alberta, personal communication). Representative helices of *M. sexta* and *L. migratoria* apoLp-III are shown. [d] Sequence obtained from Breiter et al. (1991).

of these latter peptides could be enhanced by increasing the relative hydrophobicities of specific residues (Epand et al., 1987).

The amphipathic 4K peptide is represented in the form of a helical net and as a helical wheel in Figure 6, panels A and B, respectively. Helical analysis, such as determination of hydrophobic moment and hydrophobicity per residue of the nonpolar face for the 4K peptide and related helical segments in the class of insect apolipophorins, is presented in Table 2. From the helical wheel plot it can be seen that the polar face is wide and subtends an angle of ≥180° perpendicular to the helical axis. The average hydrophobic moment of the α-helical segment of the 4K peptide (Glu 131 to Thr 164 in the native protein, Glu 1 to Thr 34 in the 4K peptide, according to SEQSEE prediction) was found to be in the range for representative helices within *M. sexta* and from *L. migratoria* apoLp-III (Table 2). The hydrophobicity per residue of the nonpolar face, on the other hand, was found to be relatively low and may offer an explanation for the inability of the peptide to interact with nonmicellar lipids. A distinct cluster of lysine residues bearing positive charges is present at the interfacial region between the polar and nonpolar faces, Lys 12, Lys 10, and Lys 28 with contribution of partial charges from His 21 and His 30. Glu 1, shown at the interface, likely does not exist in this conformation since preliminary NMR data of the structure of the 4K peptide in 50% TFE suggest that this residue is not included in the helical region. On the polar face there is a random radial distribution of charged residues. From these considerations it appears that the 4K peptide has the characteristics of both class A and G* helices (Segrest et al., 1990). However, the relevance of the charge distribution in the amphipathic α-helices of insect apolipophorins in interaction with lipids is not clear as it has been proposed that apolipophorins bind to diacylglycerol in the expanding lipophorin surface (Wang et al., 1992; Singh et al., 1992) or exposed lipoprotein surfaces (Liu et al., 1993). It has also been demonstrated that the presence of a Pro residue (Pownall et al., 1986) decreases the magnitude of the helical hydrophobic moment in a given segment of apolipoprotein. It is possible that Pro 139 (position 9 from the N-terminal end of the peptide) contributes to the poor lipid affinity.

In the helical net diagram of the 4K peptide (Figure 6A), residues on the hydrophobic face are highlighted. This is the face that makes contact with the rest of the protein in its five-helix bundle conformation in the lipid-free state. The negative charges at the N-terminal end of the helix contribute to the stability of the helix by interaction with the helical macrodipole (Shoemaker et al., 1987). The free N-terminus generated during CNBr digestion, however, may decrease the lipid affinity of the peptide. From our calculations it is also seen that the last few residues decrease the overall hydrophobicity of the peptide (data not shown) and may not be involved in lipid interaction in the native protein.

The existence of the peptide as a random coil when isolated from the rest of the molecule and in the presence of phospholipid bilayers suggests that other structural features of the intact protein play a role in maintaining the helical and structural integrity of this segment. In human apoE (which also exists as an α-helical bundle) it was shown that several interhelical salt bridges exist (Wilson et al., 1991). If such ion pairing exists in *M. sexta* apoLp-III, loss of these interactions upon isolation of the C-terminal helix may have an adverse effect on helix stability and/or lipid interaction. The presence of multiple lipid-associating domains in other known apolipoproteins [see Segrest et al. (1992)] leads us to believe that, in apoLp-III also, contributions from other domains within the tertiary structure, or helix−helix interactions, are relevant in determining the conformational stability of the terminal helix.

In conclusion it is seen that monitoring Tyr fluorescence emission and quantum yield is a useful molecular probe to detect lipid-binding ability of apoLp-III and the 4K peptide. The poor phospholipid affinity of the terminal helical segment of *M. sexta* apoLp-III, despite its propensity to form an amphipathic helix, indicates that additional features such as contributions from other regions in the molecule are essential for association with lipoproteins and/or phospholipid bilayer vesicles. Further studies are in progress to address the role of domains that may be directly involved in protein−lipid interactions of apoLp-III.

ACKNOWLEDGMENT

The authors gratefully acknowledge Mei-Yu Cai for the preparation of apoLp-III from *M. sexta*, Paul Semchuk for help with the HPLC and mass spectrometry, Leslie Hicks for sedimentation equilibrium studies and preparation of the figures, Dr. D. G. Scraba and R. Bradley for the electron microscopy, and Drs. K. Rajarathnam and J. J. Wang for critical reading of the manuscript.

REFERENCES

Anantharamaiah, G. M., Jones, J. L., Brouillette, C. G., Schmidt, C. F., Chung, B. H., Hughes, T. A., Bhown, A. S., & Segrest, J. P. (1985) *J. Biol. Chem. 260*, 10248−10255.

Breiter, D. R., Kanost, M. R., Benning, M. M., Wesenberg, G., Law, J. H., Wells, M. A., Rayment, I., & Holden, H. M. (1991) *Biochemistry 30*, 603−608.

Chervenka, C. H. (1969) in *A Manual for the Analytical Ultracentrifuge*, Spinco Division of Beckman Instruments, Inc., Palo Alto, CA.

Cole, K. D., Fernando-Warnakulasuriya, G. J. P., Boguski, M. S., Freeman, M., Gordon, J. I., Clark, W. A., Law, J. H., & Wells, M. A. (1987) *J. Biol. Chem. 262*, 11794−11800.

Cowgill, R. W. (1963) *Arch. Biochem. Biophys. 100*, 36−44.

Edelhoch, H., Perlman, R. L., & Wilchek, M. (1968) *Biochemistry 7*, 3893−3900.

Eisenberg, D., Schwarz, E., Komaromy, M., & Wall, R. (1984) *J. Mol. Biol. 179*, 125−142.

Eisinger, J. (1969) *Photochem. Photobiol. 9*, 247−259.

Epand, R. M., Gawish, A., Iqbal, M., Gupta, K. B., Chen, C. H., Segrest, J. P., & Anantharamaiah, G. M. (1987) *J. Biol. Chem. 262*, 9389−9396.

Holden, H. M., Kanost, M. R., Law, J. H., Wells, M. A., & Rayment, I. (1988) *J. Biol. Chem. 263*, 3960−3962.

Jirgensons, B. (1976) *Biochim. Biophys. Acta 434*, 58−68.

Jonas, A., Steinmetz, A., & Churgay, L. (1993) *J. Biol. Chem. 268*, 1596−1602.

Kanellis, P., Romans, A. Y., Johnson, B., Kercret, H., Chiovetti, R., Jr., Allen, T. M., & Segrest, J. P. (1980) *J. Biol. Chem. 255*, 11464−11472.

Kawooya, J. K., Keim, P. S., Ryan, R. O., Shapiro, J. P., Samaraweera, P., & Law, J. H. (1984) *J. Biol. Chem. 259*, 10733−10737.

Kawooya, J. K., Meredith, S. C., Wells, M. A., Kézdy, F. J., & Law, J. H. (1986) *J. Biol. Chem. 261*, 13588−13591.

Lakowicz, J. R. (1983) in *Principles of Fluorescence Spectroscopy*, pp 341−379, Plenum Press, New York.

Lau, S. Y. M., Taneja, A. K., & Hodges, R. S. (1984) *J. Chromatogr. 317*, 129−140.

Liu, H., Scraba, D. G., & Ryan, R. O. (1993) *FEBS Lett. 316*, 27−33.

Lund-Katz, S., Anantharamaiah, G. M., Venkatachalapathi, Y. V., Segrest, J. P., & Phillips, M. C. (1990) *J. Biol. Chem. 265*, 12217−12223.

Macquaire, F., Baleux, F., Huynh-Dinh, T., Rouge, D., Neumann, J.-M., & Sanson, A. (1993) *Biochemistry 32*, 7244−7254.

McLean, L. R., Hagaman, K. A., Owen T. J., & Krstenansky, J. L. (1991) *Biochemistry 30*, 31−37.

Pownall, H. J., Gotto, A. M., Knapp, R. D., & Massey, J. B. (1986) *Biochem. Biophys. Res Commun. 139*, 202−208.

Roth, M., Lewit-Bentley, A., Michel, H., Deisenhofer, J., Huber, R., & Oesterhelt, D. (1989) *Nature (London) 340*, 659−662.

Ryan, R. O. (1990) *J. Lipid Res. 31*, 1725−1739.

Ryan, R. O., Keim, P. S., Wells, M. A., & Law, J. H. (1985) *J. Biol. Chem. 260*, 782−787.

Ryan, R. O., Oikawa, K., & Kay, C. M. (1993) *J. Biol. Chem. 268*, 1525−1530.

Schägger, H., & von Jagow, G. (1987) *Anal. Biochem. 166*, 368−379.

Schumaker, V. N., & Puppione, D. L. (1986) *Methods Enzymol. 128*, 155−170.

Segrest, J. P., Jackson, R. L., Morrisett, J. D., & Gotto, A. M. (1974) *FEBS Lett. 38*, 247−253.

Segrest, J. P., De Loof, H., Dohlman, J. G., Brouillette, C. G., & Anantharamaiah, G. M. (1990) *Proteins: Struct., Funct., Genet. 8*, 103−117.

Segrest, J. P., Jones, M. K., De Loof, H., Brouillette, C. G., Venkatachalapathi, Y. V., & Anantharamaiah, G. M. (1992) *J. Lipid Res. 33*, 141−166.

Shoemaker, K. R., Kim, P. S., York, E. J., Stewart, J. M., & Baldwin, R. L. (1987) *Nature 326*, 563−567.

Singh, T. K. A., Liu, H., Bradley, R., Scraba, D. G., & Ryan, R. O. (1994) *J. Lipid Res. 35*, 1561−1569.

Snel, M. M. E., Kaptein, R., & de Kruijff, B. (1991) *Biochemistry 30*, 3387−3395.

Sonnichsen, F. D., Van Eyk, J. E., Hodges, R. S., & Sykes, B. S. (1992) *Biochemistry 31*, 8790−8798.

Sparrow, J. T., & Gotto, A. M., Jr. (1980) *Ann. N.Y. Acad. Sci. 348*, 187−211.

Sparrow, J. T., Sparrow, D. A., Culwell, A. R., & Gotto, A. M. (1985) *Biochemistry 24*, 6984−6988.

Stryer, L. (1966) *J. Am. Chem. Soc. 88*, 5708−5712.

Su, Y. T., & Jirgensons, B. (1977) *Arch. Biochem. Biophys. 181*, 137−146.

Suits, A. G., Chait, A., Aviram, M., & Heinecke, J. W. (1989) *Proc. Natl. Acad. Sci. U.S.A. 86*, 2713−2717.

Teale, F. W. J. (1960) *Biochem. J. 76*, 381−388.

Van der Horst, D. J. (1990) *Biochim. Biophys. Acta 1047*, 195−211.

Van der Horst, D. J., Ryan, R. O., Van Heusden, M. C., Schulz, T. K. F., Van Doorn, J. M., Law, J. H., & Th. Beenakkers, A. M. (1988) *J. Biol. Chem. 263*, 2027−2033.

Vanloo, B., Morrison, J., Fidge, N., Lorent, G., Lins, L., Brasseur, R., Ruysschaert, J.-M., Baert, J., & Rosseneu, M. (1991) *J. Lipid Res. 32*, 1253−1264.

Wang, J., Liu, H., Sykes, B. D., & Ryan, R. O. (1992) *Biochemistry 31*, 8706−8712.

Weers, P. M. M., Kay, C. M., Oikawa, K., Weintzek, M., Van der Horst, D. J., & Ryan, R. O. (1994) *Biochemistry 33*, 3617−3624.

Weintzek, M., Kay, C. M., Oikawa, K., & Ryan, R. O. (1994) *J. Biol. Chem. 269*, 4605−4612.

Wells, M. A., Ryan, R. O., Prasad, S. V., & Law, J. H. (1985) *Insect Biochem. 15*, 565−571.

Wells, M. A., Ryan, R. O., Kawooya, J. K., & Law, J. H. (1987) *J. Biol. Chem. 262*, 4172−4176.

Wilson, C., Wardell, M. R., Weisgraber, K. H., Mahley, R. W., & Agard, D. A. (1991) *Science 252*, 1817−1822.

Wishart, D. S., Boyko, R. F., Willard, L., Richards, F. M., & Sykes, B. D. (1994) *Comput. Appl. Biosci. 10*, 121−132.

Zhang, Y., Lewis, R. N. A. H., McElhaney, R. N., & Ryan, R. O. (1993) *Biochemistry 32*, 3942−3952.